# Radiolysis of bituminized radioactive waste: a comprehensive review

Lucie Millot, Hanaa Houjeij, Georges Matta, Jean-Yves Ferrandis, Didier Laux, Celine Monsanglant Louvet

EPJ Nuclear Sci. Technol. **10**, 4 (2024)

https://doi.org/10.1051/epjn/2024004

EPJ Nuclear Sciences & Technologies

Available online at:
https://www.epj-n.org

REGULAR ARTICLE

OPEN ACCESS

# Radiolysis of bituminized radioactive waste: a comprehensive review

Lucie Millot[1], Hanaa Houjeij[2,*], Georges Matta[1,2,3], Jean-Yves Ferrandis[3], Didier Laux[3], and Céline Monsanglant Louvet[2]

[1] Institut de Radioprotection et de Sûreté Nucléaire (IRSN), PSE-ENV/SPDR/USDR, F-92260 Fontenay-aux-Roses, France
[2] Institut de Radioprotection et de Sûreté Nucléaire (IRSN), PSN-RES/SCA/LECEV, F-91400 Saclay, France
[3] IES, University of Montpellier, CNRS, Montpellier, France

Received: 14 December 2023 / Received in final form: 9 February 2024 / Accepted: 21 February 2024

**Abstract.** In the realm of radioactive waste management, the impact of radiolysis on bitumen and bituminized radioactive waste also called bituminized waste product (BWP) is considered one of the most significant factors influencing structural changes and the generation of radiolysis gas bubbles. This review provides a comprehensive overview of several studies that have explored the intricate interaction between radiation and various types of bitumen, to gain a better understanding of how such waste ages when exposed to radiation. While these studies provide insights into the diverse effects of radiolysis on bitumen, they also highlight numerous unanswered questions. The absence of gas bubbles does not necessarily indicate an absence of gas production, leaving further research to be undertaken. The complexities of bitumen radiolysis offer multiple avenues for future investigation, aiming to enhance our understanding and provide comprehensive solutions for bituminous radioactive waste management. Among the studied types of bitumen, blown R85/40 bitumen and straight-run distilled bitumen with a penetration grade of 70/100 stands out due to their widespread use in immobilizing co-precipitated radioactive sludges. These bituminous matrices play an essential role in understanding the broader implications of radiolysis within the context of bituminous waste management. This review underscores the significance of further research into radiolysis and bitumen ageing, emphasizing the need for a more in-depth exploration of these complex phenomena and their implications for the long-term safety and efficacy of repositories and disposal facilities.

## 1 Introduction

The bituminization of radioactive waste is a technology widely used to immobilize and contain radioactive waste in a bitumen matrix [1,2]. The bituminized radioactive waste or bituminized waste product (BWP) is mostly classified as intermediate and low-level waste (ILW and LLW). This process provided several advantages at the time, including a low radioactivity leaching rate, assumed chemical stability and inexpensive cost [3,4]. Nevertheless, it has a number of disadvantages, notably the lack of waste volume reduction, the fire hazard, the weak resistance to biodegradation and the risk of soil contamination with nitrates [5]. One of the key issues in the radiolysis of bituminized radioactive waste is its degradation by ionizing radiation emitted by radioactive waste. In fact, this radiation has the ability to break the chemical bonds in bitumen, resulting in the production of radiolysis products such as free radicals [6]. These radicals can subsequently react with the bitumen components, resulting in the progressive chemical degradation of the material. Therefore, the radiolysis can weaken bitumen's structure, which may increase the risk of potential radionuclide leaks into the environment [7]. Another major issue is the release of radiolytic gases produced during bitumen decomposition [6]. These gases, such as hydrogen and methane, can accumulate inside waste packages and increase internal pressure. This accumulation of gases can potentially lead, in the event of a fire, to deformation or rupture of the packages, thus compromising the long-term integrity of the repository [8,9]. Understanding the radiolysis of bituminized waste is thus essential for assessing the long-term safety of repositories and disposal facilities during the operational period. This review specifically addresses the radiolytic behaviour of bituminized radioactive waste when stored and disposed of in dry, well-ventilated conditions. In this regard, the scientific community has expended an enormous effort on understanding bitumen radiolysis. However, the diversity of bitumen types, wastes, and experimental methodologies has received little attention in the literature.

* e-mail: hanaa.houjeij@irsn.fr

In the last two decades, our understanding of bitumen behaviour has significantly evolved, despite the extensive research conducted between the 1980s and 2000s [6,7,10–13]. While a wealth of data exists regarding bituminized waste materials from diverse waste-producing nations, there remains a scarcity of studies that compare the diverse applications of bitumen in the context of various radiation sources. This review aims to address this gap by examining and comparing different bituminized wastes and the various bitumen types used to embed radioactive waste. Embedding refers to the immobilization of solid waste achieved by enclosing it within a matrix material to create a distinct waste form [10]. It summarizes and appraises the effects of radiolysis on various bitumen and waste forms in order to gain better insights into bitumen ageing under irradiation. Firstly, the different types of bitumen and radioactive wastes embedded in the bituminous matrix are summarized. Then, a detailed overview of the experimental approaches used to investigate the different radiations is provided. Thereafter, the review emphasized the numerous chemical, rheological, and thermal effects on the material. Finally, the generation of radiolysis gas (gas composition, bubble formation, and swelling) is discussed.

## 2 Diversity of bituminous materials: understanding the different types of BWP

### 2.1 Bitumen type

Given the concerns about radiation and heat stability (both in terms of potential fire hazard and plasticity at elevated temperatures), bituminization is generally limited to materials with low heat production and low concentrations of alpha-emitting radionuclides. Further, some countries use bitumen as an immobilization matrix sparingly [14]. However, to produce BWPs, a diverse sort of bitumen was used.

First, according to IAEA [2], distilled bitumen is used in Switzerland, Sweden, the former Soviet Union (Ukraine and Lithuania [15]), Belgium and France. It consists of a two-stage distillation process: air distillation followed by vacuum distillation. The bitumen thus obtained contains no additives that alter its consistency [6]. Ebano 15 bitumen, grades[1] 70/100 and 80/100 bitumen are examples of this category. The nomenclature H is followed by two numbers or just two numbers corresponding to the range of softening points of this grade of bitumen. The penetration of this grade of Mexphalte is ranged between 6 and 12 1/10mm at 25 °C. H is for Hard bitumen [16].

Another method, "blowing", involves injecting air into a bituminous base heated to between 300 and 340 °C. The nomenclature R is followed by two numbers corresponding to their softening temperature and R is used for Oxidized bitumen. In this case, the first figure corresponds to the softening point and the second one is for penetration, i.e., R85/40 has a ring and ball or softening point of 85 °C and a penetration at 25 °C of 40 1/10mm. In blown bitumen, the absorbed molecular size of the asphaltenes already present in the feed increases, and new asphaltenes are formed from the maltene phase [16]. Blown bitumen or Oxidized bitumen is used in Japan, Belgium and the United States, and has been extensively studied in Belgium [17]. One of the most widely used bitumen for waste conditioning is Mexphalt R85/40.

Finally, there is the cracking bitumen "Carbasphalte 95/1" and "Carbasphalte 155/0" [16] and emulsified bitumen. Cracking bitumen is produced through the pyrogenic breakdown of heavy molecules. They have not been selected and used for embedding evaporative concentrates due to their hardness and the resulting embeddings' high fragility. However, considering research on their behaviour under ionizing radiation, this work presents the studies conducted on this bitumen. Emulsified bitumen is produced by direct injection and emulsification of bitumen in water [2,18].

Each of these methods is used in different countries according to their needs and specific bitumen applications. Bitumen is classified based on the depth to which a standard needle penetrates under specific test conditions. This needle penetration test is used to indicate the hardness of the bitumen. It is possible to plot the penetration as a function of temperature and calculate a penetration index, which is very useful for assessing the bitumen's susceptibility. The test of penetration is made based on the European standard EN 1426 and determines the depth to which a 1 mm diameter needle penetrates a sample of bitumen maintained at 25 °C under a 100 g load applied for 5 s. The result of this test is expressed in tenths of millimetres. All bitumen studied in this review is presented in Table 1 by bitumen type (distilled, blown or cracking bitumen).

### 2.2 Radioactive waste embedded in bitumen

From the 70's to 2022, bituminized literature stated numerous forms of waste embedded in a bituminous matrix [1,2,15,18,19]. Currently, according to Ojovan [18], the total volume of BWP exceeds 200 000 $m^3$.

Four waste types are identified: (i) sludge and slurry, (ii) spent ion exchange resin, (iii) liquid waste concentrates and (iv) incinerator ash. Nonetheless, the literature on this form of bitumen usage is limited. As a result, this review is concentrated on the four forms of radioactive waste stated above. These waste types are briefly detailed below. On the other hand, some nations have combined many waste streams into the bituminous matrix. For example, Table 2 presents a scenario in Sweden [15,20], where ion exchange resins, concentrates and cellulose are embedded in the bituminous matrix.

#### 2.2.1 Sludge and slurry

The purpose of this treatment is to process large quantities of radioactive liquids while producing a small quantity

[1] Bitumen grade is a combination of standardized tests (penetration, viscosity, and softening point) that ensures a certain bitumen quality.

**Table 1.** Bitumen types used in irradiation studies.

| | Distilled bitumen | Blown bitumen | Cracking bitumen |
|---|---|---|---|
| Bitumen types found in the literature | Mexphalt 10/20, 20/30, 40/50, 60/80 H80/90, 35/50, 70/100, 80/100, Ebano 15, Mexphalt 34, Mexphalt 35, | R85/40, R20/30, 40/60, R90/40, R115/15, BDN 60/90, Pionner 312, | Carbasphalte 95/1, Carbasphalte 155/0 |

**Table 2.** Waste composition of a reference package extract from SKB report in 2001 [20].

| Category | Bitumen | Ion exchange resin | Evaporator concentrate | Cellulose |
|---|---|---|---|---|
| F.05 | 95 | 130 | – | – |
| F.17 | 820 | 650 | 120 | 3.6 |
| F.18 | 960 | 600 | – | – |
| F.20 | 3420 | 4680 | – | – |
| B.05 | 150 | 50 | –* | – |
| B.06 | 150 | 50 | –* | – |
| B.20 | 5400 | 1800 | –* | – |

*Present in small quantities in the waste from Barsebäck NPP.

of waste. It consists of adding a small quantity of non-radioactive salts with a specific chemical affinity to the radionuclides in the liquid waste. This generates insoluble precipitates to which radionuclides can be attached either by co-precipitation or by adsorption. Filtration, centrifugation, or decantation are subsequently used to concentrate the sludge. Slurry, unlike sludge, does not require any extra treatment. This process of radioactive waste treatment is carried out by several nations, including France, Belgium, Russia, Ukraine [1,2,15,19], and Poland [21].

#### 2.2.2 Spent ion-exchange resin (SIERs)

In the nuclear industry, ion exchange resins are widely used to remove radioactivity from process liquids and waste streams. For example, SIERs are used for coolant purification and filtration and secondary circuits of pressurized water reactor (PWR), in moderator and primary coolant circuits of pressurized heavy water reactor (PHWR) and in feedwater and coolant purification of boiling water reactor (BWR). Such resins are mainly used in the form of organic resins, whether beads or powders. However, inorganic materials have gained an increasingly important role in the selective removal of specific radionuclides [22]. It is worth noting that some ion-exchange resins used in reactors are recycled, whereas others are for a single use. These resins are bituminized in several countries such as Finland, Sweden, and Czech Republic [1,2,15,19].

#### 2.2.3 Liquid waste concentrates

Effluent evaporation produces liquid waste concentrates with high concentrations of inactive soluble salts and low suspended particulate content. To prevent crystallization, certain concentrations are maintained heated. In several countries, including Belgium, Germany, Switzerland, Sweden, Japan, Lithuania, and Russia, these forms of liquid waste concentrations are solidified by homogeneous incorporation into bitumen [1,2,15,19].

#### 2.2.4 Incinerator ash

The volume of incineration ash produced by waste treatment is significantly reduced, yielding an inert oxide product containing some percentages of carbon as well as a radioactivity concentration in the ash. One of the issues associated with ash management is the wide size range and the presence of metals unless the trash has been pretreated prior to incineration. To avoid mechanical failure of bituminizing equipment, ash particle separation must be employed. Mixing incinerator ash with bitumen is considered by Canada [2] and Belgium [15].

### 2.3 Absorbed dose and dose rate of bituminous waste packages

The knowledge of bituminized waste absorbed doses and dose rates is essential for determining waste acceptance criteria (WAC) regarding storage and disposal facilities, as well as for studying and understanding radiolytic processes.

Sweden [20] has estimated the exposure of these bitumen waste packages over a 10 000-year period on the basis of its radionuclide inventory and package type and forecasted a cumulative dose of 0.01–0.1 MGy. For the Belgian

Eurobitum [23], average and maximum dose rates are estimated for alpha and gamma radiation for periods of 1 year, 100 years, and 100 000 years, as shown in Table 3. For instance, a maximum dose rate of 0.008 Gy/h is estimated for a period of 100 000 years. On the other hand, an absorbed dose of 4.5 MGy [24] over 200 years is estimated for French bitumen waste. Indeed, the dose rates for the French bituminized waste generated at La Hague termed STE3 (Effluent Treatment Plant 3) bituminized waste, range between 5 and 10 Gy/h. This rate is roughly a factor of ten lower after 50 years [25].

## 3 Bitumen radiation interaction

### 3.1 Phenomenology

The fundamental processes involved in the interaction between ionizing radiation and matter are shared by all organic matter and produce free radicals [26].

Under irradiation, bitumen releases $H_2$ through a radical process. Indeed, in hydrocarbons, composed solely of carbon and hydrogen, the breaking of a C-H bond produces a highly reactive H radical. The latter can rip a hydrogen atom from a neighbouring $CH_2$ group. This in turn generates new macroradicals, $H_2$ molecules as well as volatile hydrocarbons ($CH_4$, $C_2H_4$, $C_2H_6$, or $C_3H_8$) [6]. Furthermore, under anaerobic conditions, macroradicals can originate at the centre of the bitumen, and through cross-linking reactions, they will produce bridges by forming unsaturated bonds, rearrangement, or coupling with other free radicals [6,23]. Nevertheless, the presence of oxygen in the proximity of the radicals produced during irradiation is the key distinction between the core and the surface of the irradiated material. Indeed, the investigation of radio-oxidative modifications revealed that the bituminized matrix is highly sensitive to the presence of oxygen and to the irradiation factors. In particular, this ageing process may lead to a variation in the structural properties of the bitumen throughout the oxidation process, such as the development of polar oxygen species (ketones, sulfoxides, carboxylic acids, alcohols, etc.) [25]. This latter may tend to form micelles with a larger molecular weight and release $CO_2$ and CO [6]. According to a previous study [17], involving dioxygen reactions, occurred both within the surface and at a depth of the bitumen. Indeed, the evolution of the oxidized thickness appears to be proportional to the square root of the dose and inversely proportional to the dose rate for tests irradiated at low dose rates. Considering radioactive decay, the thickness of the oxidized zone after 200 years of storage can be estimated between 3.5 and 5 cm (this is detailed in 0). Moreover, data extrapolation implies that this oxidation happened further in the drum, but it is difficult to precisely determine the depth at which it occurred [25]. All the phenomena discussed above are summarized in Figure 1.

### 3.2 Radiosensitivity of different organic families

The bitumen industry uses a variety of methods to produce bitumen from the refining of bitumen. The oil firms recommend categorizing crudes based on the proportions of the following families: saturates represented in Figure 2D, aromatics (alkene, alkyne) represented in Figure 2C, resins (e.g. alkane or paraffin) represented in Figure 2B and asphaltenes represented in Figure 2A as well as to their sulphur content [16,27,28]. The analysis which determines the percentage of Saturates, Asphaltenes, Resins and Aromatics is called SARA analysis.

In the realm of radioactive waste treatment, understanding the radiosensitivity of the various organic species composing the bitumen is crucial. The component of bitumen consists of four main families: (i) saturates (ii) asphaltenes, (iii) aromatics and (iv) resins.

The term "saturates" comes from the fact that certain carbon atoms are linked to the largest possible number of hydrogen atoms [23]. Accordingly, this family includes linear alkanes which are the most radiosensitive molecules. Mouazen [29] reported that the fraction of saturates in bitumen 70/100 decreased as the absorbed dose increased during irradiation. The latter is related to the C–C bond breakage in the tertiary carbons, i.e., the carbons bonded to three other carbon atoms of alkanes [6].

Asphaltenes are extremely polar, complex aromatics with a very large molecular weight [30]. It is frequently related to the viscosity of bitumen (higher asphaltene content produces harder bitumen with lower penetration, hence higher viscosity). Indeed, asphaltene nanoaggregate can be formed via the stacking of polycyclic aromatic hydrocarbons (PAHs) branched by alkane chains [31]. Owing to the presence of heteroatoms (N, O, S), PAHs are the first site of intermolecular interaction as well as being polarizable [16,31]. With an average of six, these nano aggregates may be organized to create aggregate clusters. Asphaltene clusters can no longer expand beyond this structure, and the maximum number of nano aggregates per aggregate is predicted to be eight. Furthermore, asphaltene structure (heteroatoms, number of aromatic rings, and alkyl side chains) and percentage are essential criteria for determining the effect of radiolysis on bitumen. Indeed, Mouazen [29], Sobolev et al. [32], and Mijnendonckx et al. [30] observed an increase in the number of C=O and C=C groups, and in asphaltene content, a decrease in saturates and aromatics content, and a consistent amount of resins for the radio-oxidation process.

Resins are often referred to as "polar aromatics". Their structure is similar to that of asphaltenes, with a lower molar mass.

Aromatics are formed up of non-polar carbon chains with unsaturated (aromatic) ring systems that have a high ability to dissolve other high molecular weight hydrocarbons [16]. Aromatics are more resistant to ionizing radiation than alkanes and alkenes due to delocalized $\pi$ electrons that prevent bonds from breaking [6,23]. For the 70/100 distilled bitumen, they are the dominating proportion, accounting for between 30 and 55% of the absorbed mass and are primarily responsible for the glass transition of bitumen with non-crystallized saturates [30]. Irradiation causes aromatization (an increase in the content of unsaturated chains and aromatic rings, accompanied by a decrease in aliphatic chains), resulting in the rigidity

**Table 3.** Evolution of the average dose rates in the course of time in Eurobitum containers with average and maximum activity data extracted from [23].

| Duration | Alpha average dose rate | Alpha max dose rate | Beta/gamma average dose rate | Beta/gamma max dose rate |
|---|---|---|---|---|
| Year | Gy/h | Gy/h | Gy/h | Gy/h |
| 1 | 0.6 | 1.6 | 5 | 20 |
| 100 | 0.8 | 2.2 | 1 | 5.5 |
| 100 000 | 0.05 | 0.1 | 0.002 | 0.008 |

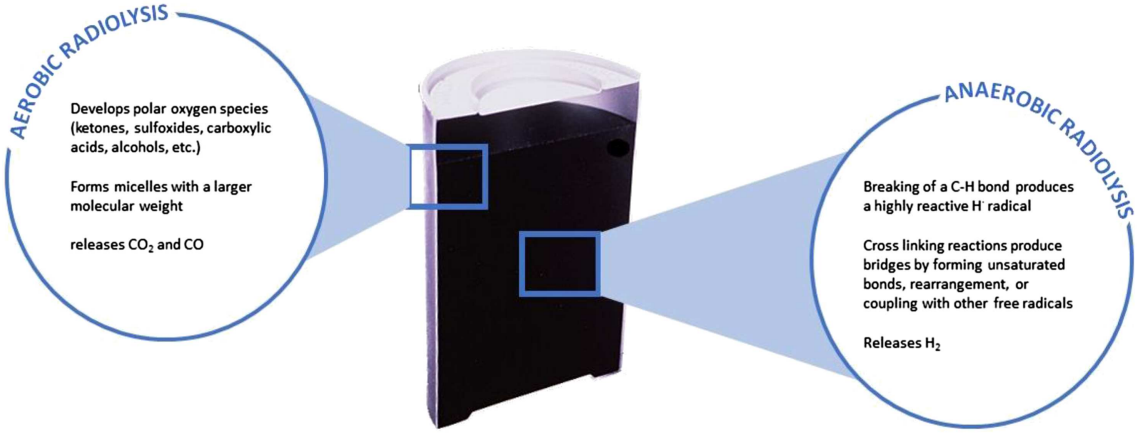


**Fig. 1.** Comparison of Aerobic and Anaerobic Radiolysis Effects on bitumen (based on data from [6,17,25,33,34]).

of the bitumen's internal structure, as reported previously [30]. Furthermore, the author showed that when the bitumen aromatizes, the masses of aromatics, resins, and asphaltenes increase, thus resulting in a more compact and denser asphaltene structure under irradiation.

## 4 Experimental setups for bitumen irradiation

To investigate these radiolytic phenomena, laboratory experiments were carried out in which bitumen was irradiated with various types of radiation (alpha, beta, and gamma). Most of these studies attempted to accelerate radiolytic phenomena in order to observe the impact of several hundred years of irradiation over short time periods.

### 4.1 Alpha radiolysis

In the early 1980s, few studies investigated the impact of alpha radiation on bitumen matrices [26,35,36]. To overcome this lack of knowledge, several studies were carried out in the same period at Los Alamos (New Mexico) [35], AERE Harwell (United Kingdom) [26] and Karlsruhe, (Germany) [36]. They focused on the production of radiolysis gas and the impact of radiation on the radiolytic yield. The experimental data are summarized in Table 4.

### 4.2 Beta irradiation

To assess the influence of beta radiation, irradiation experiments were performed employing electron gas pedals by the Commissariat à l'Énergie Atomique CEA (French Atomic Energy Commission) at the Marcoule site [37] in the 1960s. Straight-run distillation bitumen (Mexphalt 40/50 and H80/90), blown bitumen (Mexphalt R90/40 and R115/5) and cracking bitumen (95/1 and R115/15) were all investigated. Samples were irradiated using a Van de Graaff gas pedal, which produced a 1 MeV electron flux at dose rates ranging from 1 MGy/h to 100 MGy/h. Even though the employed dose rates are not representative of the real ones, the analysis of these diverse samples revealed that blown bitumen degrades less than the distillation bitumen or cracking bitumen. Besides, under such dose rates that are higher than real dose rates, a thermolysis effect can be developed. As a result, it will be difficult to distinguish between thermolysis-related alterations and irradiation-related deterioration. Similarly, it has been reported [37] that the absorbed dose rate has a considerable impact on bitumen behaviour.

### 4.3 Gamma irradiation

The most prevalent form of irradiation used to study bitumen radiolysis is gamma irradiation. Table 5 lists the different types of bitumen, the irradiation sources, the dose

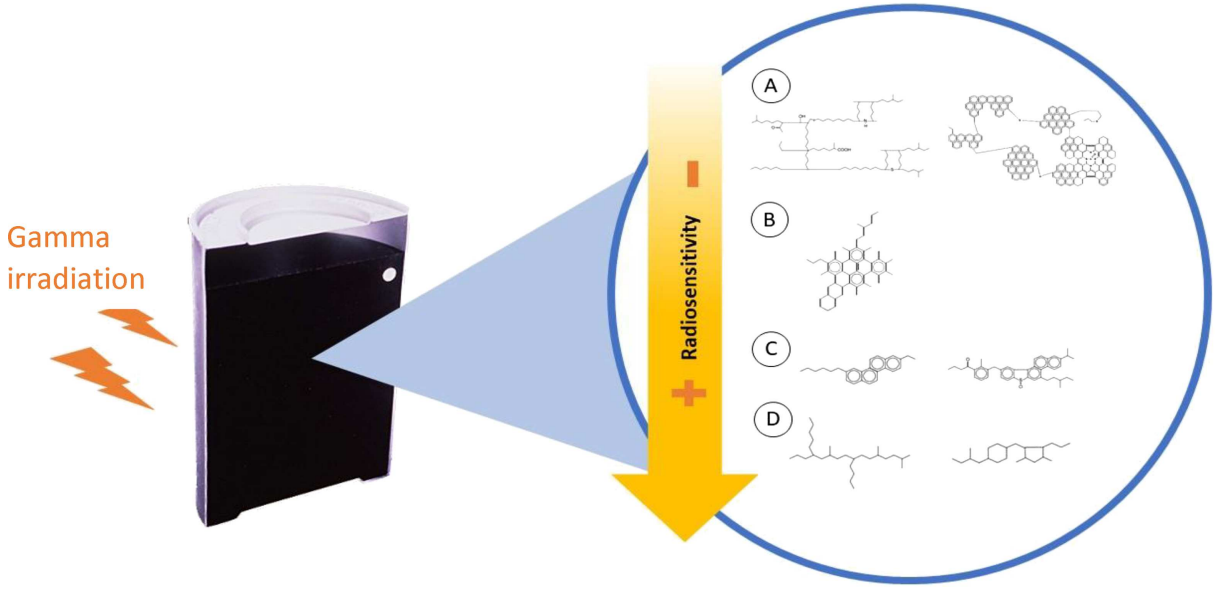


**Fig. 2.** Gamma radiosensitivity of main fraction of bitumen with some examples of molecular structures: (A) asphaltene, (B) resin, (C) aromatic and (D) saturate based on data from [16,30,31,34,38].

**Table 4.** Summary of alpha irradiation experiments by bitumen type, specific activity, absorbed dose and dose rate.

| References | Alpha source | Bitumen | Specific activity (mCi/g) | Dose rate (Gy/h) | Absorbed dose (MGy) |
|---|---|---|---|---|---|
| [35] | $^{238}PuO_2$ and $^{239}PuO_2$ | Distilled bitumen | 64 and 0.4 | Not specified[b] | Not specified |
| [26] | $^{241}Am$ | Mexphalt R85/40 | 0.80 | 90 | 0.56 |
| [36] | $Cm_2O_3$ and $PuO_2$ | Ebano 15 et Mexphalt R85/40 | 4 | 44,5[c] | 1.0–24 |

[b]The value reported in the literature is known as dosage rate, although the unit is Ci/g, which is a measure of specific activity.
[c]Calculated from the literature value 3.9 $10^7$ rad.an$^{-1}$.

**Table 5.** Summary of gamma irradiation experiments in terms of bitumen type, dose, and dose rate.

| References | Bitumen (Type or grade) | Source | Dose rate (Gy/h) | Absorbed dose (MGy) |
|---|---|---|---|---|
| [37] | 40/50, H80/90, R80/90, 95/1, 155/0 | $^{60}Co$ $^{137}Cs$ | 400–2400 1000 | 27.6 |
| [29] | 70/100 | $^{60}Co$ | 5000 | 1–7 |
| [36] | Mexphalt 34 and 35, R85/40 | $^{60}Co$ | 1000 | $34 \times 10^{-6}$–550 $\times 10^{-3}$ |
| [25] | 70/100 | $^{60}Co$ | 15 and 45 150 and 450 | 0.03 |
| [39] | 60/80, R20/30 | $^{60}Co$ | 610 1200 12 000 | 10 |

rate, and the absorbed dosage used in these studies. The tested doses ranged from 0 to 27 MGy and are represented in Figure 3. Most experiments are performed with Cobalt-60 sources. For example, for 70/100 bitumen, some experiments have been carried out on CIGAL irradiator (Conservation par Ionisation Gamma des Aliments) at CEA Cadarache and Isotron irradiator (Marseille) [25,29].

The behaviour of Mexphalt R85/40 blown bitumen under irradiation (alpha, beta and gamma) is extensively studied by several laboratories around the world [32,35]. Bitumen 70/100, which is commonly used in the French nuclear industry, is thoroughly researched, particularly with regard to gamma irradiation [29,38]. Cracking bitumen is not chosen as a radioactive waste matrix due to its hardness and the high friability of the mixtures obtained [37].

The literature [30,37] showed that absorbed doses and dose rates have a significant influence on bitumen performance. Further, Burnay [26] highlighted that, regardless of the bitumen type, one of the major conclusions is that the modifications in bitumen properties are more significant for alpha at equivalent absorbed doses. As such, it is recommended that caution must be taken while simulating alpha damage using gamma irradiation. In fact, when exposed to external gamma irradiation or 10 MeV electrons, the average $H_2$ production yield rises by a factor of 2.7.

## 5 Material properties under irradiation

The material properties define how a material responds to mechanical forces (such as strength, hardness, elasticity, plasticity, and so on) as well as changes in temperature and thermal conditions (such as thermal conductivity, thermal expansion, heat capacity, etc.). These characteristics are critical in the selection and design of materials for various applications. This section examined the effects of radiolysis on bitumen properties such as rheology, chemical, and thermal properties.

### 5.1 Chemical properties

The chemical characteristics of bitumen provide important information about its molecular composition and the types and amounts of hydrocarbons present in the material. The link between bitumen's chemical composition and physical qualities such as viscosity and viscoelasticity is critical in bitumen use [40]. Despite the bitumen composition that depends on its source and protocol of synthesis, bitumen is mostly composed of aromatic and aliphatic hydrocarbons, as mentioned previously in section 0. In this respect, many rheological and thermal properties will be determined by the quantities of these compounds. Several methods can be used to assess the organic content in natural or industrial bitumen mixtures, including C-H-O analysis, Rock-Eval pyrolysis, SARA fractionation and infrared spectroscopy [41–44].

The long-term evolution of bituminized waste drums containing salts (sludge, slurry and concentrate) is a major concern for several countries [15]. In fact, several countries are interested in both the problems of storage and disposal in the operational phase [8,9,15,23], and storage after closure after more than 100 years when the water from the host rock completely saturates the storage cells containing the bituminised radioactive waste packages [45–50].

To study long-term phenomena, one proposed approach is to use natural analogues. Indeed, a number of similarities and comparable properties are identified in the literature [3,4,41–44,51–56] between industrial (depending on the production methods, the nature of the used petroleum, etc.,) and natural bitumen. Studies on irradiated natural bitumen analogues [41–44,51–56] demonstrated that the combined effects of various alterations (leaching, microbial alteration, radiolysis) induce chemical changes such as i) an increase in the content of oxygenated compounds and hydroxyl and carboxyl functional groups; ii) a decrease in aliphatic chains and iii) an increase in aromaticity and cross-linking via oxygen bridges. Indeed, the authors [39,40,45–50,57] noticed an aromatization of molecules as well as a loss of functional groups and atoms. For instance, the H/C ratio tends to decrease on average, whereas the O/C ratio increases. Mouazen [29] reported similar results when irradiating 70/100 bitumen. The author [29] noticed that the aromatic and resin fractions increased due to the decrease in the percentage of aliphatic and aromatization of the bitumen during irradiation.

In summary, the literature [3,4,41–44,51–56] showed that industrial bitumen and natural analogues may be compared. Despite the results that appear to be similar in terms of increased aromaticity, increase in radio O/C and decrease in radio H/C, etc., natural bitumen is subjected to other phenomena (leaching alterations, microbial alterations, and radiolysis) that may alter its chemical composition [41]. Bitumen alteration by leaching phenomena is more detailed in the literature [45–50]. Thus, understanding irradiation processes on real drums would improve the forecasting of waste matrix ageing and, consequently, the simulation models used to estimate the potential fire hazards of storage and disposal facilities.

### 5.2 Rheology

One of the main physical properties relevant to the performance of bitumen is its rheology [16]. It can be evaluated regarding bitumen viscosity or complex elastic moduli. From a practical point of view, penetrometry experiments are also performed to have a rapid and qualitative estimation of bitumen behaviour.

#### 5.2.1 Viscosity

Bitumen's viscosity can be modified over time owing to physical and chemical processes such as polymerization and evaporation of volatile components. These modifications can fluctuate the bitumen viscosity over time. According to the IAEA review [2], the viscosity of blown bitumen under irradiation at ambient temperature is significantly less time-dependent than that of distilled

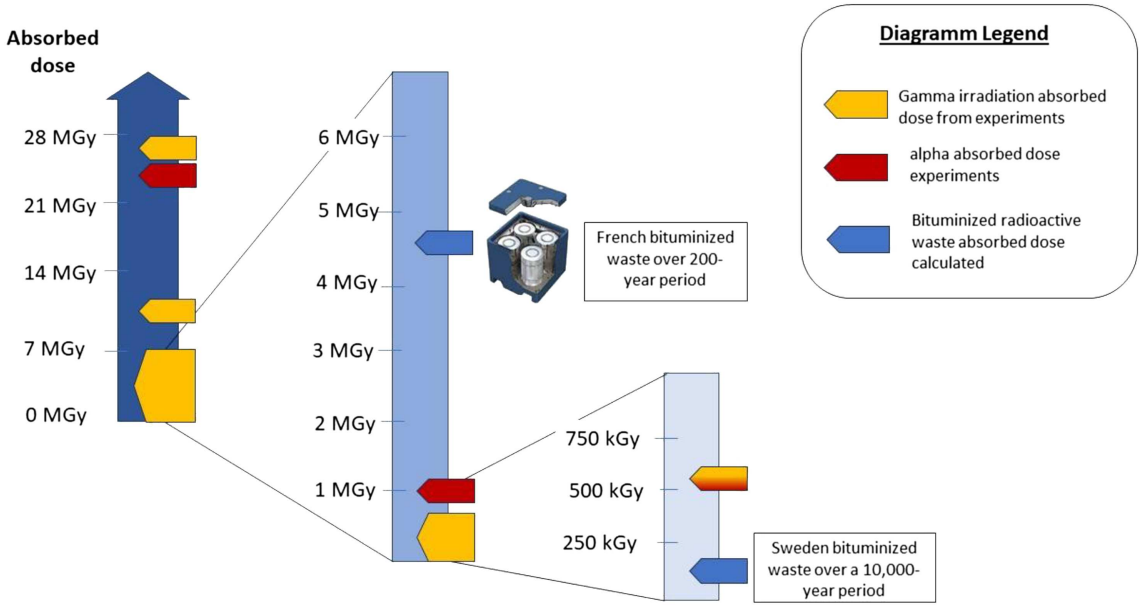


**Fig. 3.** Absorbed dose scale for bitumen experiments with alpha and beta radiation and examples of BWPs absorbed doses.

bitumen. This property of minimal time dependency of viscosity is maintained even at higher temperatures, such as 60 °C. This implies that the viscosity of blown bitumen is reasonably stable at various temperatures and is not subject to significant change over time. In contrast, the viscosity of distilled bitumen may vary considerably over time.

The viscoelastic character of blown bitumen, in particular the R85/40 bitumen, has been studied and modelled previously [58]. In this model, underwater swelling is considered rather than radiolytic swelling. On the other hand, Tabardel-Brian et al. [37] showed that blown bitumen is more resistant to degradation induced by gamma radiation, and BWPs made from blown bitumen exposed to gamma radiation exhibited an absence of volume growth. Particularly, research studies [2,26] showed that Mexphalt R85/40 bitumen cracks, whereas distillation bitumen is less viscous and swells up. Thus, the changes in viscosity as a function of irradiation are most relevant for distillation bitumen.

Mouazen's research work [29,59,60,62] provided a better understanding of the evolution of the rheological properties of 70/100 bitumen subjected to gamma irradiation. Mouazen's [29] rheological measurements were performed utilizing the stress mode on a controlled stress rheometer (ARG2, TA Instruments) fitted with an electrically heated plate (EHP) system for thermal stability and parallel plate geometry (25 mm diameter, 1 mm gap). Stress sweep experiments from $10^{-5}$ to 100 $s^{-1}$ were used to create viscosity curves in the 22–70 °C range and the corresponding shear stress was measured once steady-state flow was detected. A stabilization time of 60 s is chosen for all conditions, which was shown to be sufficient to provide a steady shear rate within 5%. Based on the obtained results, a rheo-ageing law based on the Krieger-Dougherty model was proposed, covering the entire reversibility period. This law considers the irradiation dose, the volumetric fraction of salts incorporated in the bitumen, and the temperature. Furthermore, the author [60] demonstrated that the viscosity of 70/100 bitumen changes with temperature in two regimes: (i) temperatures below 50 °C and (ii) higher temperatures. The activation energy value is determined to be 175 kJ/mol for the 22–50 °C range and 117 kJ/mol for the 50–90 °C range. These findings indicate that bitumen viscosity is more sensitive to temperature fluctuation at low temperatures than at high ones. Nevertheless, Mouazen [29] measured the viscosity of pure 70/100 bitumen and STE3 type inactive mixes (70/100 bitumen and sludge) at an absorbed dose of 5 MGy and at various temperatures (between 22 °C and 50 °C, the temperature at which 70/100 bitumen can be considered a Newtonian liquid [57], and 70 °C, the temperature corresponding to a bitumen mix's flow threshold). The results revealed that the absorbed dose also has a considerable effect on bitumen viscosity and BWRs, as summarized in Table 6.

Further, a complete study of the rheology of bitumen 35/50 [61] was carried out using ultrasonic measurement within the framework of construction and civil engineering rather than the treatment of radioactive waste. Thus, the ageing of bitumen was not considered in the latter study. To our knowledge, post-irradiation rheological studies have not yet been carried out on other distillation bitumen. Nevertheless, the dose limit for studying bitumen viscosity is one of the constraints highlighted by this review. Indeed, research studies performed by CEA [37] indicate that most of the bitumen was coked, i.e., the formation of solid coke, above a certain dose in beta irradiation (30–100 MGy). Thus, this coked bitumen was too solid to be studied with a plate micro-viscosimeter. However, those that could still soften did so at such a high degree that measurements became unfeasible. To

**Table 6.** Evolution of viscosity as a function of temperature and absorbed dose. Results from Mouazen's thesis [29].

| Dose | 70/100 | | | STE3 Bituminized waste product | | |
|---|---|---|---|---|---|---|
| | Viscosity at 22°C | Viscosity at 50°C | Viscosity at 70°C | Viscosity at 22°C | Viscosity at 50°C | Viscosity at 70°C |
| (MGy) | (Pa.s) | (Pa.s) | (Pa.s) | (Pa.s) | (Pa.s) | (Pa.s) |
| 0 | $4.40 \times 10^5$ | 940 | 56 | $1.35 \times 10^6$ | $3.67 \times 10^3$ | 220 |
| 5 | $1.18 \times 10^6$ | $3.08 \times 10^3$ | 128 | $1.10 \times 10^7$ | $18.2 \times 10^3$ | 695 |

our knowledge, no prior studies have examined equivalent phenomena in other irradiation studies. However, the authors of the study [37] indicated that, owing to high dose rates, the thermal effects could be inextricably linked with radiolysis effects.

#### 5.2.2 Bitumen hardness

Penetration is defined as the depth to which a standard needle of a specific shape penetrates vertically into a bitumen sample under a given load and temperature. The penetration test is performed by applying a specific force for a given time to the needle, followed by a free fall onto the bitumen sample. The distance at which the needle has penetrated the bitumen during a given time interval is measured and expressed in tenths of a millimetre (0.1 mm). Bitumen penetration is sensitive to temperature, bitumen composition and the presence of additives or modifiers. It is widely used to characterize bitumen consistency and quality. The penetration of bitumen is inversely related to its viscosity: the lower the penetration figure, the harder the bitumen and vice versa. The impact of irradiation is known to increase the bitumen viscosity and make it harder [2,34,57]. However, for R85/40 bitumen, the needle penetration depths reported [17] for unirradiated samples and nitrogen-irradiated samples up to 770 kGy are comparable to around 2 1/10mm. This shows that the influence of irradiation on this feature of bitumen is quite minor for this type of bitumen.

### 5.3 Thermal properties

In the case of bitumen, various thermal properties are critical for process development as well as for storage safety in the event of an accident, such as a fire. For instance, it includes softening point, glass transition temperature ($T_g$) and thermal capacity ($C_p$).

#### 5.3.1 Softening point and glass transition temperature

Both the softening point and the glass transition temperature are essential features of polymers, including bitumen. The softening point is generally associated with the thermal properties of the material, in particular its melting properties as the temperature rises. $T_g$ is defined as the temperature at which an amorphous solid becomes brittle and soft. Precisely, it is a kinetic process characterized by a change in baseline, which corresponds to a change in thermal capacity [40]. According to Lesueur [28], $T_g$ is one of the most important parameters describing the structure of a bitumen. Indeed, it is an indication of the material's stiffness at lower temperatures in bitumen containing large polymer fractions [28,59,62]. However, it is not applicable to all bitumen.

The softening point is an important input for the study of bitumen, both for BWRs produced with distillation bitumen and blown bitumen, particularly for sludge, slurry, concentrate, and incineration ash incorporation processes. Concerning blown bitumen, investigations [17] on unirradiated and irradiated BWR samples containing Mexphalt R85/40 bitumen revealed that the softening points are 126 °C and 128 °C, respectively. This implies that irradiation has little effect on the softening point. We are not aware of any studies on the effect of irradiation on other types of blown bitumen.

In the case of distillation bitumen, researchers were focusing on the evolution of the process, as demonstrated by Shon [63] in 2000. The purpose was to mix spent agricultural polyethylene PE (between 5 and 10% by mass) into 60/70 distillation bitumen. The idea was to use a bitumen matrix to encapsulate radioactive incinerator ash. This study revealed that adding 5% by weight or more of used PE to bitumen boosts the softening point above 118 °C. However, the authors say that above a certain PE loading, there is no effect on the softening point. This is due to the softening point of the used PE (about 105 °C).

In 1998, studies [64,65] were carried out on the glass transition temperatures of asphalt cement. Differential scanning calorimetry (DSC) curves showed several of these transitions, along with similarities between thermoanalytical and rheological characteristics [64,65]. This is an approach from the Strategic Road Research Program that defines certain parameters characterizing the rheological properties of bituminous cement(s). The crystallized fractions and glass transition temperature appear to be largely responsible for the physical hardening that occurs over time, and the extent of this hardening also depends on the position of $T_g$ with respect to the specified conditioning temperature. This technique was used by Mouazen [29] who highlighted two glass transitions in 70/100 distillation bitumen. Given the complexity and instability of this bitumen, three heating and cooling cycles from −90 to 100 °C were performed at a heating rate of 5 °C/min without altering the sample. The glass transition ($T_g$) values were determined during the second heating cycle. Accordingly, the maltene matrix revealed the first glass transition

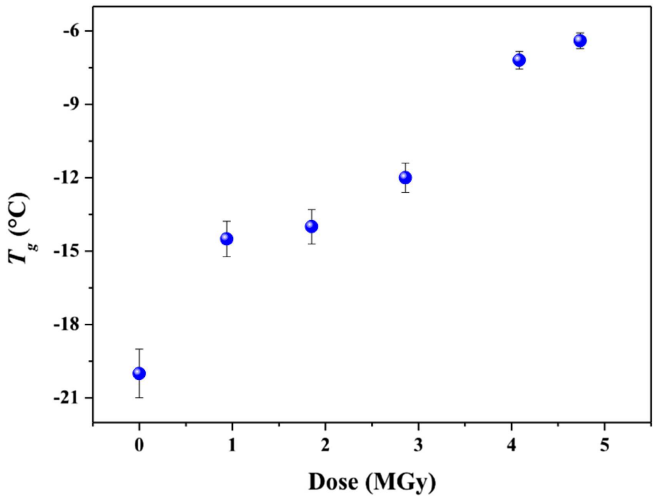


**Fig. 4.** The evolution of the glass transition temperature as a function of gamma irradiation dose for a 70/100 bitumen extracted from Mouazen thesis [29].

at approximately −20 °C, while asphaltenes revealed the second transition between 50 and 70 °C. Interactions between asphaltene aggregates were also observed at these temperatures. The author [29] irradiated this 70/100 bitumen and obtained the result shown in Figure 4. Indeed, a noteworthy trend is observed in the glass transition temperature ($T_g$) as we progress from 0 to 1 MGy, where $T_g$ increases significantly from approximately −20 °C to −14°C. Subsequently, within the range of 1–2 MGy, $T_g$ stabilizes at around −14 °C. However, between 3 MGy and 5 MGy, $T_g$ shows a linear increase, climbing from −12 °C at 3 MGy to −6 °C at 5 MGy.

To conclude, for both distilled and blown bitumen, radiolysis increases the softening point of Mexphalt 35 and Mexphalt R85/40 bitumen [2] and the glass transition ($T_g$) for 70/100 bitumen [29].

#### 5.3.2 Thermal capacity

The knowledge of $C_p$ as a function of dosage is essential for the support of the safety approach and the control of the fire risk hypotheses as well as for the propagation of a fire to a nearby package in storage settings. The literature on the thermal capacity of irradiated bitumen is quite limited. Indeed, a single research study [29] on 70/100 bitumen revealed the effect of gamma irradiation on this thermal characteristic. A modulated Differential scanning calorimetry was used for the measurements. The concept is based on the use of a linear heating rate and a sinusoidal temperature oscillation at the same time. In crucibles, 10 mg of bitumen is added and purged with nitrogen in aluminium crucibles. Measurements are carried out using inert gas scavenging to avoid interactions with the furnace environment. As a result, the thermal capacity of 70/100 bitumen increased from 0.16 J/g.°C for unirradiated bitumen to 0.49 J/g.°C for irradiated bitumen at 5 MGy.

## 6 Radiolysis gas

The formation of radiolysis gases is one of the macroscopic aspects of radiolysis events that has a significant influence on nuclear safety, particularly the fire risk [8,9]. Accordingly, in this section, the composition of radiolysis gases and the chemical species generated during the irradiation are reported, along with the different factors impacting gas composition and distribution. Thereafter, the radiolytic swelling of bitumen is presented, focusing on the impact of gas buildup inside the bituminous matrix on the mechanical properties of the material.

### 6.1 Gas composition and distribution

#### 6.1.1 Dose rate and absorbed dose

The major gas formed for both blown [26,39] and distilled [6,25,39,66] bitumen irradiated with gamma rays under oxygen or in an inert environment is hydrogen. Dushner et al. [67] demonstrated in the 1970s that the hydrogen average proportion of radiolysis gases is about 95% and is independent of the absorbed dose, irradiation settings (in an air or inert gas environment), bitumen/salt structure composition, and prior treatment. Dojiri et al. [39] reported a similar result, stating that the evolution of hydrogen is dictated only by the absorbed dose and is independent of the dose rate. It is crucial to note that the absorbed doses (10 MGy) and dose rates (610 Gy/h 1200 Gy/h and 12 kGy/h for Dojiri[39] and 1000 Gy/h for Dushner [67]) are both significant in these two experiments. Moreover, the authors [39,68] demonstrated that for BWPs composed of 60/80 distilled bitumen, the generated radiolysis gases are composed of 75–95% di-hydrogen. Simultaneously, Dojiri and his team [39] revealed an increase in the fraction of gaseous water. It should be highlighted that the addition of water as a radiolytic component is an original feature of their work.

Several studies [23,25,29,37] have demonstrated that other gases like carbon monoxide, carbon dioxide, and low hydrocarbons have evolved. Indeed, these latter gases constitute only a minor proportion of the present gas. Nevertheless, Burnay [26] showed that at doses of 3 MGy in an oxygenated atmosphere, the evolution of $CO_2$ becomes equivalent to the evolution of $H_2$ for R85/40 blown bitumen. Walczak [25] revealed similar behaviour for distilled 70/100 bitumen irradiated with an integrated dose of 30 kGy, with modest gas emissions, whereby the evolution of $CO_2$ is comparable to that of $H_2$. Moreover, the author [25] emphasized the significance of the dose rate on the speciation of the generated gases, as shown in Figure 5. Indeed, when the absorbed dose remains constant, there are variations in gas production, particularly noticeable for $H_2$, $CO_2$, and, to a lesser extent, CO. At a dose rate of 15 Gy/h, the proportions of $H_2$ and $CO_2$ produced are quite similar, at 47.7% and 48.4%, respectively. However, at 45 Gy/h, there is a significant increase in $H_2$ production (62.9%) while the volume of $CO_2$ decreases (36.2%). When the dose rate increased to 150 Gy/h, the production of these two gases returned to levels close to their initial values, with $H_2$ at 51.4% and $CO_2$ at 48.1%.

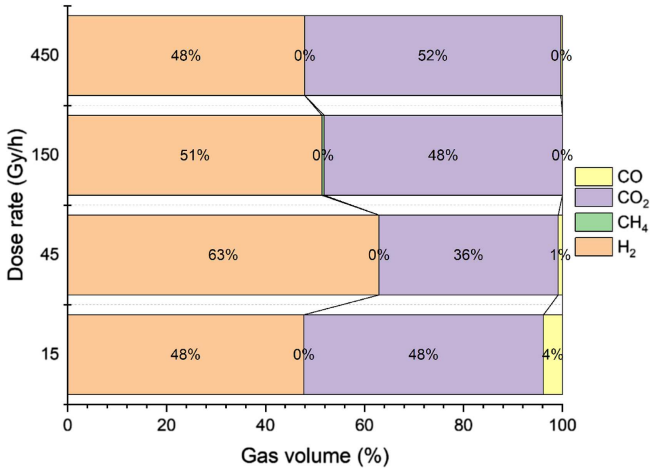


**Fig. 5.** Volume composition of radiolysis gases for 70/100 bitumen samples irradiated at varied dose rates at 30 kGy results from Walczak's thesis [25].

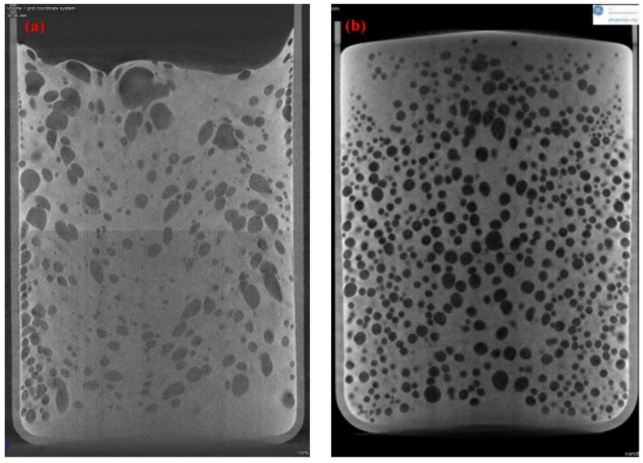


**Fig. 6.** Effect of dose rate on the shape, size and number of bubbles created, (a) BWPs at 5000 Gy/h and (b) BWPs at 400 Gy/h tomography extract from Mouazen's thesis [29].

Finally, at 450 Gy/h, $CO_2$ production slightly surpasses $H_2$ production, reaching 47.9%.

A few years later, Mouazen [29] demonstrated that for a given integrated dose (1 MGy), the dose rate impacted the distribution of bubbles inside the BWPs resulting from the STE3 plant. At a dose rate of 400 Gy/h Figure 6b, radiolysis results in the formation of uniformly spherical bubbles that are small and evenly dispersed. However, at 5000 Gy/h Figure 6a, a wide distribution of bubble sizes is observed, accompanied by irregular shapes.

The hydrogen production from a certain substance undergoing radiolysis is characterized by the *G*-value, which is the number of hydrogen gas molecules produced per 100 eV of energy. In the literature [59,62], two units are used: molecule/100 eV and mol/J, with the following converting formula [69]: $1\,\text{molecule}/100\,\text{eV} = 1036 \times 10^{-7}\,\text{mol/J}$. All findings are converted to mol/J for readability and summarized in Table 7. Nonetheless, the authors' initial values are stated in brackets.

According to Kowa [36], *G*-values for $H_2$ alpha irradiated ($0.49 \times 10^{-7}$ mol/J) is 2.7 times higher than that of beta or gamma irradiation. However, this study [36] was performed on RWF7 BWRs which consists of reprocessing concentrate (high proportion of $NaNO_3$) mixed to an R85/40 blown bitumen.

However, for 70/100 bitumen irradiated at less than 10 MGy, this *G*-value is dependent on the dose rate as demonstrated by the irradiation of 70/100 bitumen at 30 kGy at different dose rates (15, 45, 150 and 450 Gy/h) [25], as shown in Table 8. Furthermore, the author [25] showed that the radiolytic oxidation that creates $CO_2$ affects the sample's surface. Indeed, Valcke et al. [17] have also demonstrated the presence of a bitumen crust on the surface of the drum. This crust is observed to be relatively thin, less than 1 cm in thickness, due to the limited diffusion of oxygen within the bitumen. As a result, the *G*-value for $CO_2$ generation is obtained as a function of the irradiated sample surface for 70/100 bitumen and is also affected by the dose rate [25]. The author [25] explained that radiolytic oxidation exclusively affects the sample's surface, leading to the calculation of $CO_2$ production yield as a function of the irradiated sample's surface area.

To sum up, the maximum dose at which degradation may be similar, regardless of the dose rate applied to the material, is roughly 10 MGy. This degradation may correspond to a *G* value of $H_2$ in the order of 0.4–$0.5 \times 10^{-7}$ mol/J, regardless of bitumen type (distillation or blown). Therefore, it seems that there is a threshold effect over which the influence of the dose rate on an integrated dose becomes negligible. Nevertheless, the measurements presented above are carried out on a laboratory scale rather than an industrial one. For this reason, Pérot [70] reviewed the measurement of degassing in radioactive waste canisters from an operational standpoint. The measurement method entails placing the package in a sealed container and measuring the quantity of gas ($H_2$, tritium, or carbon-14) released with gas chromatography. This measurement provided an indication of the quantity of gas emitted by the package and its discharge rate. However, this method does not consider gas trapping in the bituminous matrix.

### 6.1.2 Radio-oxidation and atmosphere role

In contrast to the cross-linking seen primarily under anaerobic circumstances, irradiation in the presence of oxygen results in preferential degradation of the material [6]. During oxidizing irradiation, carbon monoxide is produced, along with other gases ($CO_2$, $CH_4$, etc.) [25,26]. This phenomenon may have a long-term impact on the package's behaviour (effect on rheology and water absorption, transport characteristics, and chemical properties) [6,39]. Several experiments [25,30] and actual situations (such as the 34-year-old Eurobitum radioactive core, where the surface layer (top 5 cm) is strongly oxidized) [17], demonstrated that oxidizing irradiation mostly affects the surface of packages, down to a thickness

**Table 7.** Hydrogen $G$-value in mol/J from various bitumen and irradiation types.

| Bitumen grade | Irradiation | Absorbed dose MGy | Dose rate Gy/h | $G(H_2)$ mol/J (molecule/100 eV) | References |
|---|---|---|---|---|---|
| R85/40 | Alpha | 24 | ~1100 | $0.49 \times 10^{-7}$(0.47) | [36] |
| 60/80 | Gamma | 0.1–10 | 1200 | $0.42 \times 10^{-7}$(0.41) | [39] |
| R20/30 | Gamma | 0.1–10 | 1200 | $0.48 \times 10^{-7}$(0.46) | [39] |
| R85/40 | Gamma | 0.5–3.11 | 100–1000 | $0.2 \times 10^{-7}$–$0.4 \times 10^{-7}$ (0.19–0.39) | [26] |

**Table 8.** $G$-value from the 70/100 distilled bitumen for different dose rate conditions, results from Walczak's thesis [25].

| Dose rate Gy/h | $G(H_2)$ mol/J (molecule/100 eV) |
|---|---|
| 15 | $0.9 \times 10^{-7}$(0.87) |
| 45 | $0.38 \times 10^{-7}$(0.37) |
| 150 | $0.34 \times 10^{-7}$(0.33) |
| 450 | $0.34 \times 10^{-7}$(0.33) |

of approximately 3.5 and 5 cm. According to Walczak [25], the bitumen radio-oxidation process is a global, two-stage phenomenon that depends on oxygen diffusion. In the first stage, the hydrocarbons constituting the material are transformed into non-acidic hydroxyl compounds. In the second stage, these compounds are oxidized in the presence of oxygen to form aromatic acids. However, further investigation regarding the presence of oxygen at higher depths in bituminized waste was reported in 2018 [17]. The key concern is whether radio-oxidation may occur within the drums, through microcracks created in the bitumen by surface oxidation, or by irradiating $NaNO_3$ crystals with oxygen (or oxygen radicals).

### 6.1.3 Impact of salts

This section will focus on bituminized waste, which contains salts (sludges, slurry, and concentrate). The impact of salts is an important aspect of sludges and slurries, in particular the presence of Nitrogen, which is a key element linked to the presence of salts in bitumen [2].

Aside from gas speciation caused by bitumen radiolysis, the presence of salt seems to be crucial in the formation or limitation of swelling of the bituminized radioactive waste. Indeed, Mouazen [29] showed that the addition of salts resulted in greater swelling compared to pure irradiated bitumen. He reported a maximum swelling (about 70%) for BWP at an integrated dose exceeding 5 MGy. This implies that a balance is achieved between gas production and removal. Marchal [66] assumed that bubbles germinate preferentially at the surface of the salts. Furthermore, it should be noted that the sludge bituminization process is both a drying and a mixing process, which implies the presence of residual water ranging from 1 to 10 wt.%, typically less than 5 wt.% [2]. Thus, the increased production of gas could be associated with both the radiolysis of water and organic content.

The salt distribution and localization in bitumen mixes suggest that gas production in the bitumen is homogenous in volume or that specific locations have higher gas production than others. Cobalt sulphide is the second most prominent insoluble salt in French STE3 BWP (9.6% of insoluble salts), with an average mass content of 2.5%, which represents a modest volume homogeneously distributed throughout the matrix. Cobalt sulphide is produced from the STE3 process (for ruthenium coprecipitation [6]) and forms cobalt sulphate and sodium sulphide. The use of cobalt sulphide showed a significant impact on the swelling of bitumen by radiolysis [71]. Indeed, the literature [71–77] has highlighted the reduction in radiolytic hydrogen production induced by inorganic sulphides, particularly cobalt sulphide. Furthermore, experiments [71] showed that significant amounts of hydrogen can be trapped in amorphous cobalt oxysulfide at ambient temperature and under pressure ranging from 0.01 MPa to 0.4 MPa. At 0.5 moles of hydrogen per mole of starting solid, the maximum levels of hydrogen trapped are predicted to be higher than 0.13 MPa. In this respect, several investigations [72–74] aimed at clarifying the mechanisms that contribute to the trapping of dihydrogen during radiolysis. Indeed, authors [74] showed that the hydrogen absorber is a combination of partly crystalline $Co(OH)_2$ and amorphous $CoS_2$ with a molar ratio of 1 $Co(OH)_2/CoS_2$. The biphasic product noted in the literature [73] is the CoSOH product, also known as basic cobalt sulphide or cobalt oxysulfide. In the presence of $H_2$, the absorber generates CoS and $Co_9S_8$. Then, $H_2S$ can be formed when the removed amorphous $CoS_2$ interacts strongly with $H_2$. Further, the literature [71] demonstrated that the addition of inorganic substances (sodium nitrate, sodium thiosulfate, cobalt hydroxide, and elemental sulphur) to a cobalt sulphide hydrogen absorber ($CoS_2 + Co(OH)_2$ combination) significantly enhances the trapping of hydrogen. The hydrogen absorber reacts with $H_2$ spontaneously, creating water and another cobalt sulphide, CoS (or $Co_9S_8$). This absorber response is required to allow $H_2$ to further reduce the inorganic additives. Whatever the additive, the amount of $H_2$ trapped increases, although at a considerably slower rate. In the instance of $Co(OH)_2$, the trapping reaction

is a quantitative two-step mechanism that involves the production of cobalt metal. In the presence of sodium nitrate, sodium thiosulfate, or elemental sulphur, the absorber and additives are reduced concurrently within a few days, resulting in the generation of gases ($NH_3$, $N_2$, or $H_2S$) that must be captured in the case of industrial uses. On the other hand, $CoS_5$, a cobalt polysulfide, is synthesized, which has a stronger hydrogen trapping capacity than $CoS_2$. Even though the first reaction rate is substantially slower owing to the greater amount of hydrogen in the air. The impact of radiolysis on cobalt sulphide salt has been investigated in previous studies [75,76]. Pichon et al. [76] showed that amorphous cobalt hydroxo-sulphide $CoS_xO_yH_z$ acts as a hydrogen scavenger independently of radiolysis. Radiolytic hydrogen is rapidly produced by irradiation, whereas hydrogen scavenging by cobalt hydroxo-sulphide is a slower phenomenon. Moreover, Loussot [73,74] investigated the impact of $CoS_xO_yH_z$ on radicals produced during hydrocarbon radiolysis in combinations of dodecane and $CoS_xO_yH_z$ at doses ranging from 0.3 to 4 MGy. Indeed, if cobalt hydroxo-sulphide is a radical interceptor, it should reduce the amount of alkenes, heavy products, and hydrogen generated by radiolysis. However, the author [76] reported that the compositions and quantities of the generated alkenes and heavy products are similar in the presence and absence of solid according to the analysis of the organic phases. Only hydrogen generation decreased in the presence of $CoS_xO_yH_z$. Besides, the author stated [76] that the solid only interacts with water through the following chemical reaction (Eq. (1)).

$$8\mathrm{CoSOH} + \mathrm{Co(OH)_2} + 5\mathrm{H_2} = \mathrm{Co_9S_8} + 10\mathrm{H_2O}. \quad (1)$$

Further, Pichon [76] suggested that the germination of $Co_9S_8$ from CoSOH is a specific mechanism that remains unknown. Indeed the author [76] noted that $Co_9S_8$ grows via reaction steps that occur at the surface of grains covered with Co9S8 seeds (adsorption of hydrogen molecules on the $Co_9S_8$ surface, interface reaction) and in the grain core (diffusion of reaction intermediates into the $Co_9S_8$and CoSOH phases). Unlike Loussot [73,74], Pichon [76] suggested that future research should focus on the desorption of $H_2S$ and $H_2O$ from the $Co_9S_8$ surface.

### 6.2 Swelling of radiolysis bituminized waste

Irradiation-induced swelling of bituminized waste products is influenced by the dose rate, absorbed dose, bitumen type, waste nature, loading, ultimate water content, sample size, and packaging [2]. In this respect, a preliminary investigation [11] showed that bubbles or cracks may emerge, depending on the type of bitumen (blown or distilled). Indeed, experiments on pure bitumen [11] demonstrated that after gamma-irradiation, distilled Mexphalt M35 bitumen generated bubbles, whereas oxidized Mexphalt R85/40 blown bitumen promoted cracks or fracture development, as shown in Figure 7. The presence of cracks in R85/40 during radiolytic swelling is confirmed by Burnay [26].

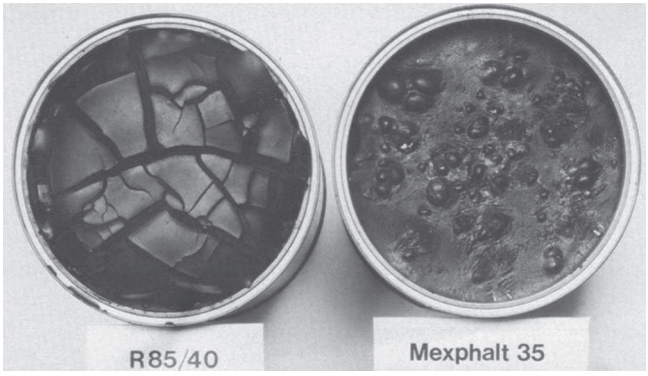


**Fig. 7.** Appearance of specimens of R85/40 and Mexphalt 35 after irradiation [11].

Mouazen [29] demonstrated radiolysis bubble generation in 70/100 bitumen. However, for bitumen 70/100, the literature [6] indicated that a minimum dose of 30 kGy is required for the first radiolysis bubbles to appear in Figure 8. Indeed, the CEA has demonstrated that the swelling of 70/100 bitumen begins following an initial latent phase [6]. During this phase, hydrogen ($H_2$) produced by radiolysis accumulates within the bitumen matrix until it reaches its saturation concentration, which occurs at the 30 kGy threshold. Eventually, the bitumen stabilizes as the bubbles formed through nucleation grow sufficiently large to rise to the surface due to buoyancy.

Phillips et al. [11] demonstrated for distillation bitumen Mexphalt 35 and blown bitumen R85/40 that the amount of swelling that occurs is affected by both the dose rate and the physical size of the sample, as well as more evident parameters such as absorbed dose, bitumen type, waste type, and volume. Indeed, when considering a consistent sample size, swelling tends to escalate with a higher dose rate. However, swelling diminishes as the physical size of the sample decreases, resulting in an increase in the surface-to-volume ratio. Mouazen et al. [60] reported the same results for 70/100 bitumen. Further, Mouazen and his team [59,60,62] demonstrated that bitumen swells at an almost constant rate of roughly 14% per MGy up to 3 MGy, after which it stabilizes at around 50–55%, indicating that a state of equilibrium between gas production and evacuation has been reached. Both authors [11,60] emphasized that radiolytic swelling studies on small samples are difficult to apply to waste streams in storage or disposal conditions.

To satisfy safety criteria, simulation tests for materials in drums are devised. Several models are proposed on the basis of a Newtonian fluid exhibiting rheology evolution over time, including the basic $IL^2$ model [11], the bubble growth model [11] and Marchal's bubble population development model [66,78]. The first two models are particularly useful for studies with tiny samples, but Marchal's model is useful for massive objects such as radioactive waste containers.

Given the complexities of the phenomenon at hand, measurements on real drums provide a better understanding of the occurrences and, as a result, enhance the

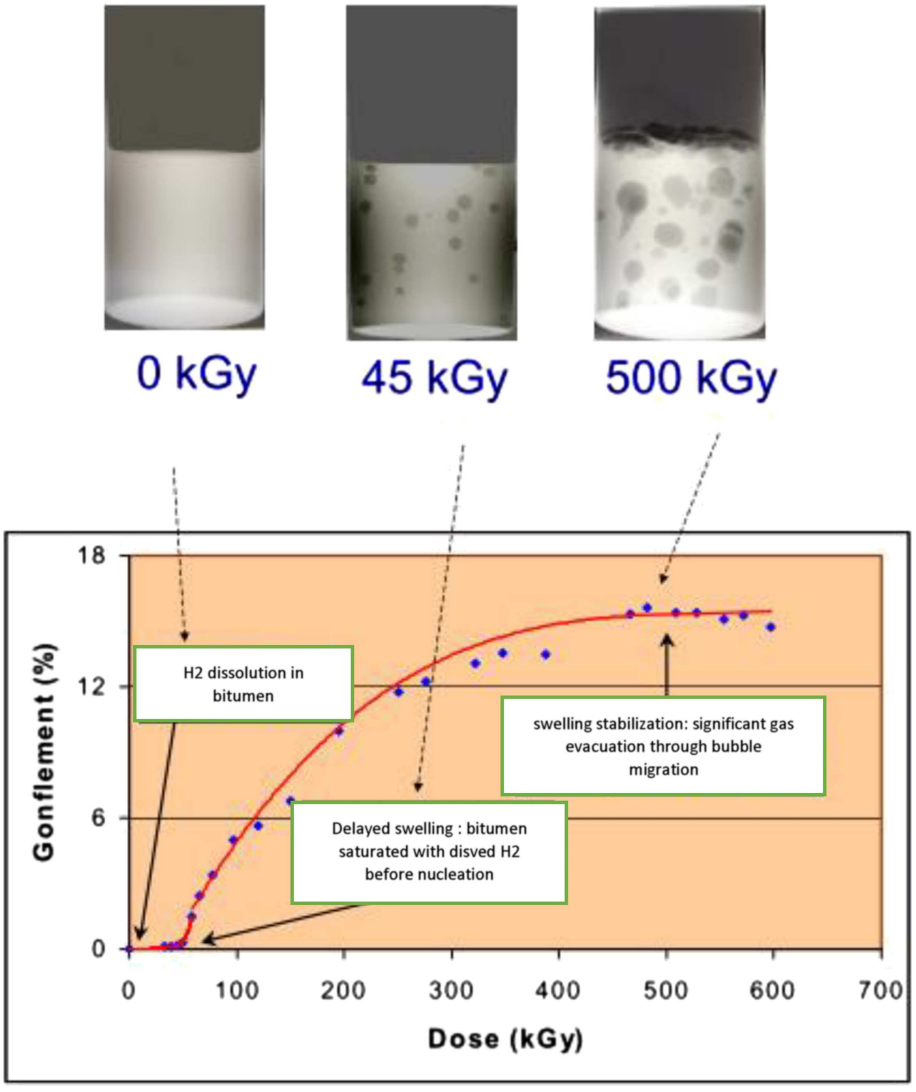


**Fig. 8.** Study of swelling of 70/100 bitumen under irradiation from 2004 CEA report [6].

proposed models. Hence, non-destructive methods like muon tomography are increasingly being explored [79,80]. The existence of radiolysis gases may be detected using this approach, which is based on the use of cosmic muons. This approach, according to Dobrowolska [79], may detect up to 2 litres of dihydrogen in bitumen.

## 7 Conclusion and future perspectives

This review investigated the effects of radiolysis on various bitumen (blown and distilled bitumen) and waste forms (sludge and slurry, SIERs, liquid waste concentrate, and incinerator ash) to gain a better understanding of bitumen ageing under irradiation. Both varied bitumen types and radioactive waste immobilized in bitumen were examined, in terms of real dose rate and absorbed dose. The experimental methodologies used to perform various forms of radiation are summarized with particular emphasis on the chemical, rheological, and thermal consequences of the studied material. Finally, particular attention is paid to the generation of radiolysis gas as well as to the evolution of gas composition, bubble formation, and swelling. In this regard, the most widely studied bitumen are R85/40 blown bitumen and 70/100 distilled bitumen. Other types of radioactive waste (incinerator ashes and SIER) received relatively little attention compared to bituminized sludge.

Blown bitumen, such as R85/40, showed poor radiosensitivity, whereas distilled bitumen 70/100 exhibited considerable swelling and changes in gas speciation under irradiation. These effects are directly related to the bitumen manufacturing process (blowing oxidizes the bitumen to a much greater extent), the dose rate, and the absorbed dose. For both bitumen types, the findings of the various investigations showed that there is a threshold effect beyond which the influence of the dose rate on an integrated dose becomes minimal. It is believed that a dose in the order of 10 MGy can be interpreted as the maximum dose at which deterioration will be comparable,

independently of the dose rate given to the material. This implies an $H_2$ $G$-value of $0.4–0.5 \times 10^{-7}$ mol/J, regardless of the bitumen grade. Regarding the generation of acid gases such as $N_2$, $NH_3$, or $H_2S$ during bitumen radiolysis, the existing literature provides only limited information, suggesting the potential for a more comprehensive study in this area.

The study of the influence of radiolysis on material characteristics, in particular rheology and thermal studies, seemed not always accessible or feasible. Moreover, it underscores the difficulty of applying radiolytic swelling investigations on small samples to waste streams in storage or disposal conditions. Furthermore, real-time direct observation of radiolytic bubbles is not possible because of bitumen opacity. In this context, exploring the feasibility of non-destructive methods, such as ultrasonic approaches, as a means of detecting radiolysis bubbles, monitoring them in real-time during gamma irradiation and/or a temperature increase, and deriving insights on the evolution of rheology represents an interesting approach to improve knowledge on these bituminous materials. Work under the ARISE project (Suivi ultrAsonore des gaz de Radiolyse des enrobés bItuméS lors d'incEndie) is currently being carried out in collaboration between IRSN (Department of Radioactive Sites and Waste Assessment[2] and IRMA facility of the Laboratory of Experimental Research on the Performance of Equipment and Ventilation[3]) and the Institut d'Electronique et des Systèmes (IES, University of Montpellier, CNRS).

This knowledge, together with precise gas speciation and an estimate of the radiolysis gas flow during a temperature increase, would improve current models, particularly fire models. Besides, from an operational point of view, techniques such as muon tomography are of potential interest for quantifying the gas trapped in the drums and for predicting the exact quantity of gas released in the event of a fire.

## Funding

We received a grant from CNRS through its interdisciplinary programs (MITI) and from IRSN through its exploratory projects. The project (ARISE: Suivi ultrAsonore des gaz de Radiolyse des enrobés bItuméS lors d'incEndie) was selected in the framework of the (CNRS/IRSN) call for proposal "Matériaux, santé et mesures: au cœur des défis du nucléaire".

## Conflicts of interest

The authors declare that they have no competing interests to report.

## Data availability statement

The authors confirm that the associated data of this review are available within the article in the references section.

## Author contribution statement

L. Millot: Funding acquisition, writing & editing, original draft. H. Houjeij, C. Monsanglant Louvet, D. Laux, J.-Y. Ferrandis: Funding acquisition, writing – review & editing. G. Matta: Writing – review & editing.

## References

1. IAEA, Bituminization of radioactive wastes (1970)
2. IAEA, Bituminization processes to condition radioactive wastes, 352 (1993)
3. B. Nagy, Role of organic matter in the Proterozoic Oklo natural fission reactors, Gabon, Africa, Geology, 0–3 (1993)
4. J.C. Petit, Natural analogues for the design and performance assessment of radioactive waste forms: a review, J. Geochem. Explor. **46**, 1 (1992)
5. S.V.Stefanovsky et al. "Nuclear waste forms." Geological Society, London, Special Publications **236.1**, 37 (2004)
6. J. Sercombe, Dossier de référence bitume: Synthèse des connaissances sur le comportement long terme des colis bitumés (2004)
7. C. Tiffreau, M.F. Libert, P.P. Vistoli, J. Sercombe, Dossier De Synthese Sur Le Comportement a Long Terme Des Colis: Dossier Operationnel Bitume (2004)
8. ASN, Revue externe sur la gestion des déchets bitumés Rapport final (2019)
9. IRSN, Avis relatif au dossier Projet Cigéo – Dossier d'Options de Sûreté (2017)
10. C.M. Jantzen, W.E. Lee, M.I. Ojovan, 6 – Radioactive waste (RAW) conditioning, immobilization, and encapsulation processes and technologies: overview and advances, in *Woodhead Publishing Series in Energy, Radioactive Waste Management and Contaminated Site Clean-Up* (Woodhead Publishing, 2013), pp. 171–272
11. D.C. Phillips, J.W. Hitchon, D.I. Johnson, J.R. Matthews, The radiation swelling of bitumens and bitumenised wastes, J. Nucl. Mater. **134**, 2 (1984)
12. S. Camaro, Rapport technique: Effets des rayonnements à long terme sur les enrobés (1992)
13. M.Porto et al. "Bitumen and bitumen modification: A review on latest advances." Applied Sciences **9.4**, 742 (2019)
14. D.G. Bennett, J.J.W. Higgo, and S.M. Wickham. "Review of waste immobilisation matrices." Nirex Limited, United Kingdom (2001)
15. V. Wasselin, M. Maître, I. Kutina, Deliverable 9.5: Overview of issues related to challenging wastes (2022)
16. J. Read, D. Whiteoak. The shell bitumen handbook. Thomas Telford, 2003.
17. E. Valcke, F. Rorif, S. Smets, Ageing of EUROBITUM bituminised radioactive waste: An ATR-FTIR spectroscopy study, J. Nucl. Mater. **393**, 175 (2009)
18. Immobilisation of radioactive waste in bitumen, *Chapter 18 of: An Introduction to Nuclear Waste Immobilisation* (Elsevier, 2109), https://doi.org/10.1016/B978-0-08-102702-8.00018-2

[2] Unité d'expertise des sites et des déchets radioactifs (USDR).

[3] Laboratoire d'Expérimentations sur le Comportement des Equipements et de la Ventilation (LECEV). The IRMA facility is part of the LECEV's BOREE experimental platform.

19. L. Abrahamsen-Mills, J.S. Small, *Chapter 1 – Organic-containing nuclear wastes and national inventories across Europe, in The Microbiology of Nuclear Waste Disposal* (Elsevier, 2021), pp. 1–20
20. M. Pettersson, M. Elert, Charaterisation of bitumenised waste in SFR 1 (2001)
21. L. Fuks, I. Herdzik-koniecko, K. Kiegiel, A. Miskiewicz, Methods of thermal treatment of radioactive waste, Energies **15**, 375 (2022)
22. IAEA, Application of ion exchange processes for the treatment of radioactive waste and management of spent ion exchangers (2002)
23. K.Mijnendonckx, et al. "DELIVERABLE 1.3." (2018)
24. IRSN, Comportement physico-chimique des fûts d'enrobé bitumineux (2018)
25. I.Walczak. "Détermination des produits organiques d'ltérations chimiques et radiochimiques du bitume." Applications aux enrobés bitumes, PhD thesis, Institut National des Sciences Appliquées de Lyon, 2000
26. S.G. Burnay, Comparative evaluation of $\alpha$ and $\gamma$ radiation effects in a bitumenisate, Nucl. Chem. Waste Manag. **7**, 107 (1987)
27. D. Lesueur, La Rhéologie des Bitumes: Principes et Modification, Rhéologie **2**, 1 (2002)
28. D. Lesueur, The colloidal structure of bitumen: Consequences on the rheology and on the mechanisms of bitumen modification, Adv. Colloid Interface Sci. **145**, 42 (2009)
29. M. Mouazen, Évolution Des Propriétés Rhéologiques Des Enrobés Bitume, Vers Une Loi Vieillissement/Viscosité, Diss. École Nationale Supérieure des Mines de Paris (2011)
30. K. Mijnendonckx, N.M. Bassil, S. Nixon, A. Boylan, N. Leys, *Organic Materials and their Microbial Fate in Radioactive Waste*, (Elsevier Inc., 2021)
31. L. De Bock, S. Vansteenkiste, and A. Vanelstraete. "Categorisation and analysis of rejuvenators for asphalt recycling." A. De Swaef, Woluwedal 42–1200 (2020)
32. I.A. Sobolev, A.S. Barinov, M.I. Ojovan, N.V. Ojovan, I.V. Startceva, Z.I. Golubeva, Long term behaviour of bitumen waste form, Mat. Res. Soc. Symp. Proc. **608**, 571 (2000)
33. M. Ferry, Y. Ngono, Energy transfer in polymers submitted to ionizing radiation: A review, Radiat. Phys. Chem. **180**, 109320 (2021)
34. Andra, Colis d'enrobés bitumineux produits à partir d'effluents traités dans la STE3 (Orano/La Hague), https://inventaire.andra.fr/families/colis-denrobes-bitumineux-produits-partir-deffluents-traites-dans-la-ste3-oranola-hague
35. S.T. Kosiewicz, Gas generation from the alpha radiolysis of bitumen, Nucl. Chem. Waste Manag. **1**, 139 (1980)
36. S. Kowa, N. Kerner, D. Hentschel, W. Kluger, Investigations of the alpha radiolysis, No. KFK-3241, Kernforschungszentrum Karlsruhe GmbH (1983)
37. R. Tabardel-brian, J. Rodier, G. Lefillatre, Essais d'irradiation de bitume et d'enrobés bitumineux par Centre de Production de Plutonium de Marcoule, Rapport CEA-R-3730 (1969)
38. E.Chailleux, F. Hammoum. "La structure chimique des bitumes pétroliers." L'actualité chimique sous l'égide de la Société Chimique de France 385 (2014)
39. S. Dojiri, H. Matsuzuru, N. Moriyama, Safety evaluation of asphalt products, (I): Radiation decomposition of asphalt products, J. Nucl. Sci. Technol. **14**, 134 (1977)
40. P. Redelius, H. Soenen, Relation between bitumen chemistry and performance, Fuel **140**, 34 (2015)
41. P. Landais, Organic geochemistry of sedimentary uranium ore deposits, Ore Geol. Rev. **11**, 3 (1996)
42. R.F. Meyer, E.D. Attanasi, P.A. Freeman. "Heavy oil and natural bitumen resources in geological basins of the world: Map showing klemme basin classification of sedimentary provinces reporting heavy oil or natural bitumen." US Geol. Surv. Open-File Rep2007-1084 (2007)
43. K. H.Hellmuth, (1989). The long-term stability of natural bitumen (No. STUK-B-VALO–59). Finnish Centre for Radiation and Nuclear Safety (STUK).
44. P. Holliger, et al. "Organic matter and uraninite from the Oklo natural fission reactors: natural analogue of radioactive waste containing bitumen and UO2 irradiated fuel." EUR (Luxembourg) (1993)
45. Y. Chen et al. Investigation of bituminized waste products swelling behavior due to water uptake under free leaching conditions: Experiments and modeling. Int. J. Numer. Anal. Methods Geomech. **47**, 3351 (2023)
46. J. Sercombe, B. Gwinner, C. Tiffreau, B. Simondi-Teisseire, F. Adenot, Modelling of bituminized radioactive waste leaching. Part I: Constitutive equations. J. Nucl. Mater. **349**, 96 (2006)
47. B. Gwinner, J. Sercombe, C. Tiffreau, B. Simondi-Teisseire, I. Felines, F. Adenot, Modelling of bituminized radioactive waste leaching. Part II: Experimental validation, J. Nucl. Mater. **349**, 107 (2006)
48. M.I. Ojovan, N.V. Ojovan, Z.I. Golubeva, I.V. Startceva, A.S. Barinov, Aging of the bitumen waste form in wet repository conditions, Mat. Res. Soc. Symp. Proc. **713**, 713 (2002)
49. K.P. Zakharova, O.L. Masanov, Bituminization of liquid radioactive wastes. Safety assessment and operational experience, At. Energy **89**, 135 (2000)
50. A.S. Barinov, I.A. Sobolev, M.I. Ozhovan, Mechanisms of removal of components of liquid radioactive-wastes as a function of the salt filling of bituminous compounds, At. Energ. **65**, 977 (1988)
51. B. Nagy, F. Gauthier-Lafaye, P. Holliger, D.W. Davis, D.J. Mossman, J.S Leventhal, J. Parnell, Organic matter and containment of uranium and fissiogenic isotopes at the Oklo natural reactors, Nature **354**, 472 (1991)
52. K.-H. Hellmuth, Natural analogues of bitumen and bituminized radioactive waste, No. STUK-B-VALO-58, Finnish Centre for Radiation and Nuclear Safety (1989)
53. F. Gauthier-Lafaye, P. Holliger, P.-L. Blanc, Natural fission reactors in the Franceville basin, Gabon: A review of the conditions and results of a 'critical event' in a geologic system, Geochim. Cosmochim. Acta **60**, 4831 (1996)
54. W.R. Alexander, H.M. Reijonen, I.G. Mckinley, Natural analogues: Studies of geological processes relevant to radioactive waste disposal in deep geological repositories, Swiss J. Geosci. **108**, 75 (2015)
55. H. Hidaka, T. Sugiyama, M. Ebihara, P. Holliger, Isotopic evidence for the retention of 90Sr inferred from excess 90Zr in the Oklo natural fission reactors: Implication for geochemical behaviour of fissiogenic Rb, Sr, Cs and Ba, Earth Planet. Sci. Lett. **122**, 173 (1994)
56. J. Parnell, H. Kucha, P. Landais, *Bitumens in Ore Deposits* (Springer Berlin, Heidelberg, 2012)
57. N.K. Gulieva, G.M. Gatamkhanova, I.I. Mustafaev, radiation resistance of bituminous waterproofing materials, High Energy Chem. **54**, 336 (2020)
58. N. Mokni, S. Olivella, X. Li, S. Smets, E. Valcke, A. Mariën, Deformation of bitumen based porous material:

Experimental and numerical analysis, J. Nucl. Mater. **404**, 144 (2010)
59. M. Mouazen et al., Caractérisation rhéologique de bitumes 70/100 utilisé comme matrice de confinement de déchets radioactifs, 44ème Colloque annuel du Groupe Français de Rhéologie, Nov 2009, Strasbourg, France (2011)
60. M. Mouazen, A. Poulesquen, F. Bart, J. Masson, M. Charlot, B. Vergnes, Rheological, structural and chemical evolution of bitumen under gamma irradiation, Fuel Process. Technol. **114**, 144 (2013)
61. N. Larcher, Contribution à la caractérisation des matériaux au comportement viscoélastique par méthode ultrasonore Application aux matériaux bitumineux, Diss. Limoges (2014)
62. M. Mouazen, A. Poulesquen, F. Bart, B. Vergnes, Effect of $\gamma$ irradiation on nuclear bituminized waste products (BWP): X-ray microtomography and rheological characterization, J. Nucl. Mater. **419**, 24 (2011)
63. J.S. Shon, S.H. Lee, H.S. Park, K.J. Kim, D.K. Min, The improvement of the mechanical stability and leachability of bituminized waste form of radioactive ash by addition of reused polyethylene, Korean J. Chem. Eng. **18**, 668 (2001)
64. P.M. Claudy, J.M. Létoffé, D. Martin, J.P. Planche, Thermal behavior of asphalt cements, Thermochim. Acta **324**, 203 (1998)
65. J.P. Planche, P.M. Claudy, J.M. Létoffé, D. Martin, Using thermal analysis methods to better understand asphalt rheology, Thermochim. Acta **324**, 223 (1998)
66. A. Marchal, Modélisation du gonflement radiolytique d 'enrobés bitumineux (2015)
67. H. Duschner, W. Schorr, K. Strake, Generation and diffusion of radiolysis gases in bituminized radioactive waste, Radiochim. Acta **137**, 133 (1977)
68. B.L. Anderson, M.K. Sheaffer, L.E. Fischer, Hydrogen Generation in TRU Waste Transporation Packages Office of Nuclear Material Safety and Safeguards, No. UCRL-ID-138352. (Lawrence Livermore National Lab., 2000)
69. F. Crumiere, Études de l'effet de TEL lors de la radiolyse de l'eau: rendements radiolytiques de l'hydrogène moléculaire, Diss. Nantes (2012)
70. B. Pérot et al., The characterization of radioactive waste: a critical review of techniques implemented or under development at CEA, France, EPJ Nucl. Sci. Technol. **4**, 3 (2018)
71. D. Lambertin, C. Caudit Coumes, F. Frizon, C. Joussot-Dubien, Matériau pour le piégeage d'hydrogène, procédé de préparation et utilisations, Patent EP2367627A1 (2009)
72. D. Chartier, C. Joussot-Dubien, C. Pighini, E. Sciora, F. Bouyer, Hydrogen trapping: Synergetic effects of inorganic additives with cobalt sulfide absorbers and reactivity of cobalt polysulfide, Int. J. Hydrogen Energy, **37**, 13594 (2012)
73. C. Loussot et al., Trapping of radiolytic hydrogen by amorphous cobalt oxysulfide, J. Nucl. Mater. **359**, 238 (2006)
74. C. Loussot, P. Afanasiev, M. Vrinat, H. Jobic, P.C. Leverd, Amorphous cobalt oxysulfide as a hydrogen trap, Chem. Mater. **18**, 5659 (2006)
75. C. Pichon, N. Millard-Pinard, F. Valdivieso, A. Chevarier, M. Pijolat, P.C. Leverd, Effect of cobalt hydroxo-sulphide on organic material radiolysis, J. Nucl. Mater. **362**, 502 (2007)
76. C.Pichon,Inhibition de la production d'hydrogène radiolytique dans les déchets nuclèaires de type enrobés bitumineux: étude de l'interaction entre l'hydrogène et l'hydroxosulfure de cobalt. PhD thesis, Ecole Nationale Supérieure des Mines de Saint-Etienne, 2006.
77. D. Chartier et al., Evidence for H2S gas as an intermediate species in the reaction mechanism of trapping hydrogen by cobalt disulfide, Int. J. Hydrogen Energy **36**, 12121 (2011)
78. A. Marchal, B. Vergnes, A. Poulesquen, R. Valette, Competitive growth and rising of bubbles in a yield stress fluid. Consequences on the macroscopic swelling of bitumen drums, J. Nonnewton. Fluid Mech. **234**, 162 (2016)
79. M.Dobrowolska et al. "A novel technique for finding gas bubbles in the nuclear waste containers using muon scattering tomography." Journal of Instrumentation **13.05**, P05015 (2018)
80. N.Mori et al. "Feasibility study of detection of high-Z material in nuclear waste storage facilities with atmospheric muons." 34th International Cosmic Ray Conference (ICRC2015). Vol. 34 (2015)

**Cite this article as:** Lucie Millot, Hanaa Houjeij, Georges Matta, Jean-Yves Ferrandis, Didier Laux, Céline Monsanglant Louvet. Radiolysis of bituminized radioactive waste: a comprehensive review, EPJ Nuclear Sci. Technol. **10**, 4 (2024)